Available online at www.sciencedirect.com
SCIENCE DIRECT
Biochimica et Biophysica Acta 1758 (2006) 248–258
BIOCHIMICA ET BIOPHYSICA ACTA
BBA
http://www.elsevier.com/locate/bba

Temperature and pressure effects on structural and conformational properties of POPC/SM/cholesterol model raft mixtures—a FT-IR, SAXS, DSC, PPC and Laurdan fluorescence spectroscopy study

Chiara Nicolini [a], Julia Kraineva [a], Monika Khurana [a], Nagarajan Periasamy [a], Sérgio S. Funari [b], Roland Winter [a,*]

[a] University of Dortmund, Department of Chemistry, Physical Chemistry I-Biophysical Chemistry, Otto-Hahn-Straße 6, D-44227 Dortmund, Germany
[b] Hasylab, c/o DESY, Notkestrasse 85, D-22607 Hamburg, Germany

Received 21 December 2005; received in revised form 24 January 2006; accepted 26 January 2006
Available online 20 February 2006

Abstract

We report on the effects of temperature and pressure on the structure, conformation and phase behavior of aqueous dispersions of the model lipid "raft" mixture palmitoyloleoylphosphatidylcholine (POPC)/bovine brain sphingomyelin (SM)/cholesterol (Chol) (1:1:1). We investigated interchain interactions, hydrogen bonding, conformational and structural properties as well as phase transformations of this system using Fourier transform-infrared (FT-IR) spectroscopy, small-angle X-ray scattering (SAXS), differential scanning calorimetry (DSC) coupled with pressure perturbation calorimetry (PPC), and Laurdan fluorescence spectroscopy. The IR spectral parameters in combination with the scattering patterns from the SAXS measurements were used to detect structural and conformational transformations upon changes of pressure up to 7–9 kbar and temperature in the range from 1 to about 80 °C. The generalized polarization function (*GP*) values, obtained from the Laurdan fluorescence spectroscopy studies also reveal temperature and pressure dependent phase changes. DSC and PPC were used to detect thermodynamic properties accompanying the temperature-dependent phase changes. In combination with literature fluorescence spectroscopy and microscopy data, a tentative *p*,*T* stability diagram of the mixture has been established. The data reveal a broad liquid-order/solid-ordered (l_o+s_o) two-phase coexistence region below 8±2 °C at ambient pressure. With increasing temperature, a $l_o+l_d+s_o$ three-phase region is formed, which extends up to ~27 °C, where a liquid-ordered/liquid-disordered (l_o+l_d) immiscibility region is formed. Finally, above 48±2 °C, the POPC/SM/Chol (1:1:1) mixture becomes completely fluid-like (liquid-disordered, l_d). With increasing pressure, all phase transition lines shift to higher temperatures. Notably, the l_o+l_d ($+s_o$) phase coexistence region, mimicking raft-like lateral phase separation in natural membranes, extends over a rather wide temperature range of about 40 °C, and a pressure range, which extends up to about 2 kbar for $T=37$ °C. Interestingly, in this pressure range, ceasing of membrane protein function in natural membrane environments has been observed for a variety of systems.
© 2006 Elsevier B.V. All rights reserved.

Keywords: Lipid bilayer; Model raft mixture; Phase transition; Pressure; SAXS; DSC; PPC; FT-IR

1. Introduction

Lipid bilayer systems are valuable model systems for biological membrane. They provide a variety of polymorphic phases, depending on their molecular structure and environmental conditions, such as the water content, pH, ionic strength, and temperature [1–6]. The importance to understand not only the physical behavior of simple one-component systems, but also of heterogeneous membranes is due to the importance to understand many aspects of the biological membranes, such as membrane mechanical and thermotropic properties, lateral diffusion of membrane components and the existence of segregated membrane domains with distinct lipid compositions [7–9]. Formation of lipid domains is a mere consequence of the many-particle nature of biological membranes.

Simple, one-component saturated phospholipids often exhibit two thermotropic lamellar phase transitions, a gel to gel

* Corresponding author.
E-mail address: roland.winter@uni-dortmund.de (R. Winter).

0005-2736/$ - see front matter © 2006 Elsevier B.V. All rights reserved.
doi:10.1016/j.bbamem.2006.01.019

($L_{\beta'}/P_{\beta'}$) pretransition and a gel to liquid-crystalline (L_α or l_d) main transition at a higher temperature T_m. In the fluid-like L_α-phase, the acyl chains of the lipid bilayers are conformationally disordered, whereas in the gel phases, the chains are more extended and ordered [1,2,10]. In recent years, studies carried out on binary mixtures combining cholesterol with different saturated and unsaturated phosphatidylcholines showed the coexistence of a cholesterol-enriched "intermediate" phase, often called liquid-ordered (l_o) phase, which coexists with a cholesterol-depleted liquid-crystalline or gel phase over a wide range of temperatures and sterol contents [11,12]. Other studies have also examined the phase behavior of cholesterol-containing ternary mixtures, generally containing an unsaturated lipid like phosphatidylcholine and a saturated lipid like sphingomyelin [13–17]. Such lipid systems are supposed to mimic distinct liquid-ordered lipid regions, called "rafts", which seem to be also present in cell membranes. They are rich in sphingomyelin and cholesterol and they are thought to be important for cellular functions such as signal transduction and the sorting and transport of lipids and proteins [18–21]. Such "artificial rafts" could be expected to mimic some features of mammalian plasma membranes.

In this study, we explored the temperature and pressure dependent structure, phase behavior and fluidity of such a canonical lipid raft model system, the POPC/SM/Chol (1:1:1) mixture, using Fourier transform-infrared (FT-IR) spectroscopy, small-angle X-ray scattering (SAXS), differential scanning calorimetry (DSC), pressure perturbation calorimetry (PPC) and fluorescence spectroscopy using Laurdan as dye. FT-IR spectroscopy is a non perturbing technique that monitors molecular vibrations and thus operates on a very short time scale. It has been extensively shown in the literature that many IR spectral parameters, particularly the frequencies, widths, intensities, shapes and splitting of IR bands, are very sensitive to the structural and dynamical properties of membrane lipid molecules [22–32]. Additionally, in our study, we used the SAXS technique that allows to follow changes of membrane structural properties [33]. Besides these two techniques, we also applied thermodynamic methods to detect temperature-dependent phase changes, DSC and PPC. The latter is a rather new tool that measures the heat consumed or released by the sample after sudden small pressure jumps of a few bar, yielding precise values of the apparent coefficient of thermal expansion of the lipid bilayer [34,35]. It was already shown by Heerklotz [34] that DSC and PPC together are able to detect thermotropic changes in membrane order in ternary lipid systems. The emission spectrum of the environmentally sensitive fluorescence probe Laurdan (6-dodecanoyl-2-dimethyl-aminonaphtalene) was used to detect changes of phase behavior of the lipid bilayer system as a function of temperature and pressure. The spectral changes of the emission spectrum of Laurdan are generally quantified by the so-called generalized polarization function (*GP*). The measured *GP* values of our system reflect the overall phase behavior and fluidity of the membrane as a function of temperature and pressure.

The rationale for using pressure as an additional experimental variable in studies of biomolecular systems next to temperature has already been discussed by a number of authors (see, e.g., [36–39]). Hydrostatic pressure has essentially been used as a physical parameter for studying the stability and energetics of membranes and proteins, but also because high pressure is an important feature of certain natural membrane environments and because the high pressure phase behavior of biomolecules is of biotechnological and pharmacological interest. Temperature has been one of the most often used parameters to study the thermodynamic, structural and dynamic properties of membranes. A change in temperature of a system leads to changes of the thermal energy and density at the same time, whereas pressure dependent studies at constant temperature introduce only changes in density and change intermolecular separations of the system, hence providing additional information about the energetics and phase behavior of the system without disturbing thermally activated processes. Compared to other biomolecules such as proteins or DNA, lipid bilayers have been shown to respond most sensitively to hydrostatic pressure [36–39]. Considerable knowledge exists about pressure effects on simple, one-component lipid bilayer systems, very little is known about complex lipid mixtures, however [38–52]. Hence, by using SAXS at a synchrotron facility, DSC, PPC, FT-IR and fluorescence spectroscopy we have determined the structure and temperature–pressure phase diagram of POPC/SM/Chol (1:1:1) in a temperature range from ~1 to 70 °C and in a pressure range up to 9 kbar. Up to these pressures, the solvent, water, is still in the liquid state at these temperatures.

2. Materials and methods

2.1. Sample preparation

1-Palmitoyl-2-oleoyl-*sn*-glycero-3-phosphatidylcholine (POPC) and bovine brain sphingomyelin (SM) were purchased from Avanti Polar Lipids (Birmingham, AL), cholesterol (Chol) from Sigma-Aldrich (Steinheim, Germany). The lipids were used without further purification. The POPC/SM/Chol lipid mixtures were prepared by first dissolving the required amounts of lipids in chloroform/methanol (4:1). The solvent was then completely removed under vacuum using a Speed Vac Sc 110 (Savant, Farmingdale, NY, USA) before adding water (D_2O or H_2O). Homogeneous lipid dispersions were obtained after five freeze–thaw vortex cycles. Depending on the method, either large unilamellar or multilamellar vesicles have been prepared.

2.2. FT-IR spectroscopy

The lipids were dissolved at a concentration of 20% (w/w) in D_2O. The FT-IR spectra were recorded with a Nicolet MAGNA 550 spectrometer equipped with a liquid nitrogen cooled MCT (HgCdTe) detector. For the pressure-dependent measurements, the infrared light was focussed by a spectral-bench onto the pin-hole of a diamond anvil cell (DAC) with type IIa diamonds [32,53,54]. Each spectrum was obtained by co-adding 512 scans at a spectral resolution of 2 cm^{-1} and was apodized with a Happ–Genzel function. The sample chamber was purged with dry carbon dioxide free air. Powered α-quartz was placed in the hole of the steel gasket of the DAC and changes in pressure were quantified by the shift of the phonon band of quartz appearing at 695 cm^{-1} [54]. The temperature dependent measurements were carried out using a cell with CaF_2 windows separated by 50 μm teflon spacers. An external circulating

water thermostat was used for the pressure- and temperature-dependent measurements to control the temperature within 0.1 °C. The equilibration time before recording spectra at each temperature and pressure was 15 min.

2.3. Synchroton small-angle X-ray scattering

The X-ray diffraction data were collected at the Soft Condensed Matter Beamline (A2) of the DORIS storage ring, Deutsches Elektronen-Synchroton (DESY), Hamburg, Germany. The SAXS measurements were performed using X-rays of 8.27 keV energy (wavelength, λ, of 1.5 Å), a 1 m sample-detector distance, and a charge-couple device based detector (MarCCD). Typical exposure times were 60 s. We used a high-pressure X-ray sample cell, suitable for studies up to about 7 kbar at temperatures up to 80 °C, which was previously described [55]. Diffraction intensity versus reciprocal spacings (s, $s=2\sin\theta/\lambda$, where 2θ is the scattering angle) plots were obtained by radial integration of the 2D CCD images using the software FIT2D by A. Hammersley. The incident and transmitted beam intensities were recorded and used to normalize the data. The mesophase structure and the corresponding lattice constants were determined from the positions of the low-angle Bragg reflections. The lamellar lattice constant a_{lam} of the lamellar phases was calculated from the measured reciprocal spacing $s_{lam}=n/a_{lam}$ (with order of reflection $n=1, 2,\ldots$).

2.4. Differential scanning and pressure perturbation calorimetry

The dried lipid films were prepared as described above, and then suspended in 150 mM NaCl, 100 mM sodium phosphate buffer at pH 7.4 by gentle vortexing. Large unilamellar vesicles were produced by five freeze–thaw cycles followed by 25 passages through two stacked Nucleopore polycarbonate membranes of 100 nm pore size in a miniextruder. The samples were kept at 70 °C during the extrusion procedure. The measurements were performed on a VP DSC calorimeter from MicroCal (Northampton, MA). The sample cell of the calorimeter was filled with 0.5 mL of lipid dispersion, at a concentration of 30 mg/mL, while the reference cell was filled with a matching aqueous solution. All the measurements were performed at a scan rate of 20 °C/h. C_p values are given with respect to the reference cell. For comparison, measurements have also been performed for MLV preparations, and similar data have been obtained.

PPC measurements of the apparent coefficient of thermal expansion, α, were performed on the same sample after the DSC measurements, using the MicroCal pressurizing cap (Northampton, MA) [34,35]. A nitrogen gas pressure of ~5 bar was applied to the samples (30 mg/mL) during all PPC cycles. The effective scan rate was 20 °C/h. Under the same experimental conditions, a set of reference sample-buffer, buffer–buffer and water–water measurements was carried out each time [56].

2.5. Fluorescence spectroscopy

The emission spectrum of the environmentally sensitive fluorescence probe Laurdan (6-dodecanoyl-2-dimethyl-aminonapthalene) was used to decipher the phase behavior of the lipid bilayer system. Vesicles containing 1:1:1 molar ratio of POPC, SM and Chol were prepared together with the Laurdan fluorophore. After co-dissolving the lipids, cholesterol and fluorophore, the solvent chloroform was removed by a flow of nitrogen gas. Then, the samples were dried under high vacuum pumping for several hours to completely remove the remaining solvent. The remaining dry film was then resuspended in water, vortexed and sonicated for 15 min in a bath-type sonicator (Bandelin SONOREX RK100SH). Finally, several freeze–thaw cycles were applied to achieve a better homogeneity of the vesicle preparation. The final concentration of lipid vesicles in the samples used for the fluorescence measurements was 0.3 mmol/L and that of the fluorescent probe was ~0.5 μmol/L. The final vesicle solution contained a 1:550 fluorophore to lipid mixture on a molecular basis. At these low fluorophore levels, no significant perturbation of the lipid bilayer structure has been observed. The fluorescence spectroscopic measurements were performed using a K2 multifrequency phase and modulation fluorometer with photon counting mode equipment (ISS Inc., Champaign, Il). The temperature was controlled to ±0.1 °C by a circulating water bath. The spectral changes of the emission spectrum of Laurdan are generally quantified by the so-called generalized polarization function, which is defined as $GP=(I_B-I_R)/(I_B+I_R)$, where I_B and I_R are the fluorescence intensities at 440 nm (characteristic for an ordered, gel phase state environment) and 490 nm (characteristic for a fluid, liquid-crystalline lipid state), respectively [57]. Hence, GP values range from −1 to +1. In phase coexistence regions, the GP values exhibit values typical for fluid (liquid-disordered) and gel-type (liquid-ordered) domains. Hence, the measured GP values of our system reflect the overall phase behavior and fluidity of the membrane as a function of temperature and pressure.

3. Results and discussion

3.1. Temperature- and pressure-dependent FT-IR spectroscopic measurements

FT-IR spectroscopy was used to yield information about the conformational and molecular order of the acyl chains as well as structural changes at the interfacial region of the lipid system POPC/SM/Chol (1:1:1) in excess D_2O. The positions and intensities of IR absorption bands were analyzed to monitor the conformational properties of the lipid system [28,32,58]. The carbon hydrogen stretching vibrations give rise to bands in the spectral region between 2800 and 3100 cm^{-1}. The CH_2 antisymmetric stretching mode at ~2920 cm^{-1} and the CH_2 symmetric stretching mode at ~2850 cm^{-1} are the strongest bands that can be observed in lipid IR spectra. The position of these bands are conformation sensitive and thus give qualitative information about temperature- and pressure-induced changes of the *trans/gauche* ratio in the lipid acyl chains. The analysis of the C═O stretching mode at 1800–1700 cm^{-1} is used for the analysis of changes in the level of hydration of the lipid carbonyl group at the polar/apolar interface. The C═O band can be fitted with three Gauss–Lorentz functions and the peak areas can be evaluated to determine relative hydration changes in the interfacial region of the lipid bilayer. Analysis of the band by Fourier self-deconvolution gives rise to three overlapping bands centered at ~1744, ~1730 and ~1712 cm^{-1}, which can be assigned to the stretching vibrations of free carbonyl groups that are not involved in hydrogen bonding, and to simple and multi-hydrogen-bonded C═O groups whose vibrations are red-shifted to lower wavenumbers, respectively.

Fig. 1A shows the symmetric CH_2 stretching frequency as a function of temperature. As the temperature increases, the wavenumber of the symmetric CH_2 vibration at ~2849 cm^{-1} increases overall by ~2 cm^{-1} due to increasing elastical repulsive interactions between the lipid chains, indicating a transition from a largely ordered to a conformationally disordered phase. The peak position of the C═O stretching mode in Fig. 1B and the corresponding relative intensity of the band at 1744 cm^{-1}, representing the population of water-free carbonyl groups in the lipid head-group region, shown in Fig. 1C, exhibit two changes of the slope of $\tilde{\nu}(T)$. A first one at ~6 °C which indicates a transition to a more disordered phase, probably from a s_o+l_o phase to a three-phase region $l_o+l_d+s_o$, and a second one at ~27 °C, which indicates the disappearance of solid domains and formation of a l_d+l_o

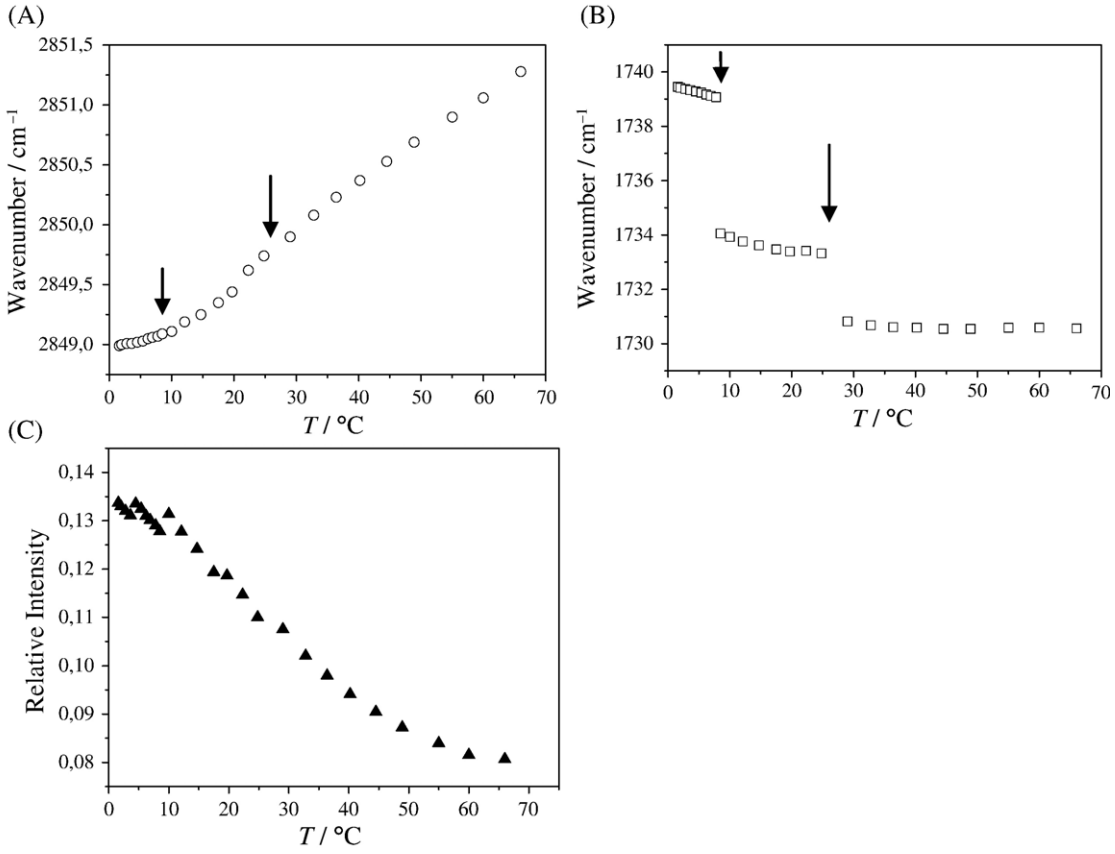

Fig. 1. Temperature dependence of (A) the CH_2 symmetric stretching mode wavenumber and (B) the C═O stretching mode wavenumber of POPC/SM/Chol (1:1:1) in excess D_2O. (C) Temperature dependence of the relative intensity of the band at 1744 cm^{-1}. This band represents the population of water-free carbonyl groups in the lipid head-group region.

two-phase coexistence region. A l_d+l_o two-phase coexistence region in this temperature region (23 and 37 °C) has been observed in fluorescence microscopy and spectroscopy [13] measurements, which help in the identification of phases in our study. The assignment of phases is also based on the results obtained from the other techniques applied (see below). At higher temperatures, we would expect to detect a further transition to an all fluid-like, l_d-phase. However, minor differences in the hydration level between fluid-like phases can probably not be resolved with sufficient accuracy with this method [32]. Also, the symmetric CH_2 stretching vibration wavenumber shows changes at similar temperatures, indicated here by changes in the slope of $\tilde{\nu}(T)$ only (Fig. 1A), which is expected for transitions between two or three coexisting phases.

The pressure dependence of the symmetric CH_2 stretching band and of the C═O stretching mode at different temperatures (15, 25, 45 and 66 °C) are shown in Fig. 2. Over most of the pressure range studied, the frequency of the CH_2 stretching wavenumber varies almost linearly with increasing pressure. Pressure induces a linear blue shift, which is generally observed when elastic repulsive forces dominate the system [58,59]. Changes in slope indicate phase transitions, are sometimes difficult to detect however, in particular for phase transitions between phases that exhibit small changes in conformational properties, only.

At 15 °C, we detect an increase of the wavenumber of ~6 cm^{-1} with increasing pressure up to 8 kbar. At ~900 bar, the curve shows a small change of the wavenumber of the symmetric stretching mode, which is probably due to the pressure-induced $l_o+l_d+s_o$ to l_o+s_o transition. The maximum of the C═O stretching vibration at 15 °C shows no significant change upon pressurization. Here, the $l_o+l_d+s_o$ to l_o+s_o transition is not detected, probably due to the low concentration of l_d domains. At the higher temperatures of 25 and 45 °C, we observe several phase changes, respectively. At 25 °C, a first transition, probably from a $l_o+l_d+s_o$ to l_o+s_o phase, which occurs at ~1100 bar (Fig. 2C, D), and at 45 °C a transition from the l_o+l_d to the $l_o+l_d+s_o$ phase at ~900 bar, as can be inferred from drastical changes in the C═O stretching mode, only. Fig. 2 also shows transitions at 25 °C from the two-phase region l_o+s_o to a gel (s_o) phase at ~4.2 kbar (Fig. 2C) and one at 45 °C to a l_o+s_o phase at ~3 kbar (Fig. 2E, F). A third transition to an all solid (s_o) phase might be indicated in a slight change in slope of $\tilde{\nu}(T)$ or the 45 °C measurement at ~4.8 kbar (Fig. 2E). The transitions from an all-fluid to l_o+l_d and $l_d+l_o+s_o$ phase coexistence regions were detected at the higher temperature of 66 °C at pressures of ~2.1 and ~2.8 kbar, respectively (Fig. 2G, H).

Owing to the fact that the detected conformational changes of this kind are often quite small and – depending on the type and concentration of the different coexisting phases – are not always detectable with sufficient accuracy in the high-pressure

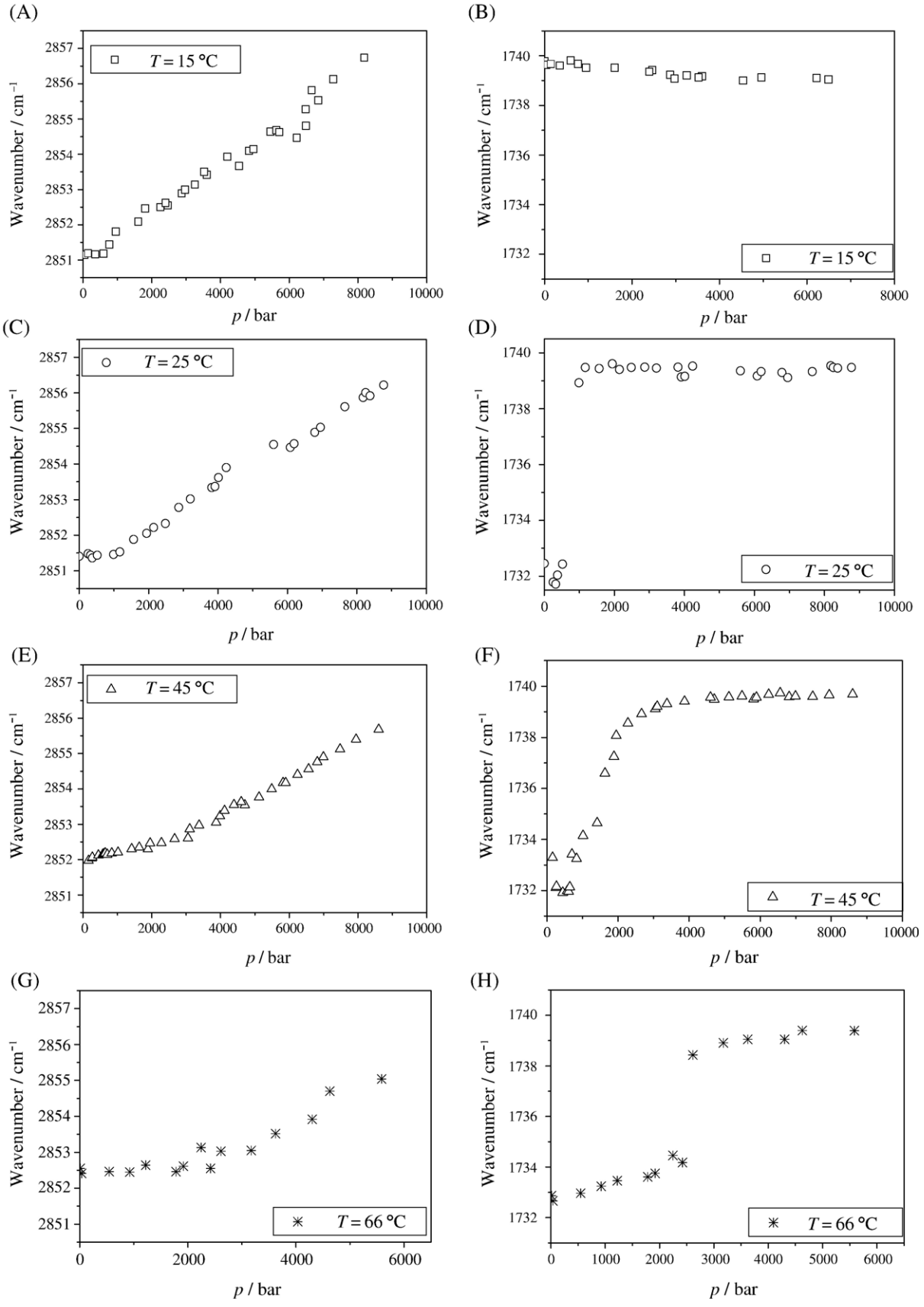

Fig. 2. Pressure dependence of the CH_2 symmetric stretching mode and the C═O stretching mode wavenumber of POPC/SM/Chol (1:1:1) in excess D_2O at different temperatures (15, 25, 45 and 66 °C).

sample environment of the diamond anvil cell to build up a *p*,*T*-phase diagram, and, in addition, are often hampered by the superimposed elastic effects on the position of bands, we combine the results of the FT-IR spectroscopy data with SAXS data, complemented by DSC/PPC and fluorescence spectroscopic measurements to yield sufficient information to build up a *p*,*T* stability diagram of the system.

3.2. Temperature- and pressure-dependent synchrotron small-angle X-ray scattering experiments

The positions of Bragg reflections in the small-angle scattering region were analyzed to determine the topology of the lipid mesophases and the average lattice constants of the corresponding structures. SAXS diffraction patterns of the three component system POPC/SM/Chol (1:1:1) in D_2O at different temperatures from 1.3 to 63 °C are depicted in Fig. 3A. The Bragg reflections display a ratio of diffraction spacings of 1:2, which is typical for lamellar phases. Probably, owing to a weak interbilayer coupling of domains, no different lattice constants are observed for coexisting phases. The average lamellar lattice constant *a* as obtained from the Bragg reflections are displayed as a function of temperature in Fig. 3B. The average lattice constant of the lamellar structures decreases by 2.8 Å with increasing temperature. At ~2 °C, *a* has a value of 71.5±0.8 Å, which probably represents the average lamellar spacing in the l_o+s_o ordered-phase. Above about 8 °C, *a* decreases continuously up to about 43 °C, where an all l_d-phase is reached with a minimum *a* value of 68.5±0.8 Å. Due to the continuous character of the transition, a small change in small-angle diffraction pattern is observed in passing the l_o+s_o to $l_o+l_d+s_o$ region at 23 °C, i.e., a similar temperature region as detected in the corresponding FT-IR spectra.

SAXS patterns at different temperatures (15, 25, 45 and 65 °C) of the same lipid mixture from 1 bar up to 5500 bar at 300–400 bar intervals have also been measured (for example, see Fig. 3C). The average lamellar lattice constant *a* is plotted for these temperatures as a function of pressure in Fig. 4. The drastic increase of *a*(*p*) in the l_d phase region with increasing pressure is probably essentially due to a straightening of the lipid acyl chains. At 15 °C, two barotropic transitions can be identified by characteristic changes of the *a*-spacings, probably a $l_o+l_d+s_o$ to l_o+s_o and the l_o+s_o to s_o transition, occurring at pressures of ~1000 and ~3100 bar, respectively (Fig. 4A). The estimated error bars in determining the transition pressures amount to about 200 bar. The slight decrease of the lamellar lattice constant in the s_o phase with increasing pressure might be due to a reduction in the interlamellar water layer. At 25 °C, only one transition is clearly visible, the transition from the $l_o+l_d+s_o$ to the l_o+s_o phase, which occurs at about 1500 bar (Fig. 4B). A second one to the s_o phase region may be indicated by a change to a negative slope of *a*(*p*) around 3.5 kbar. At 45 °C, the

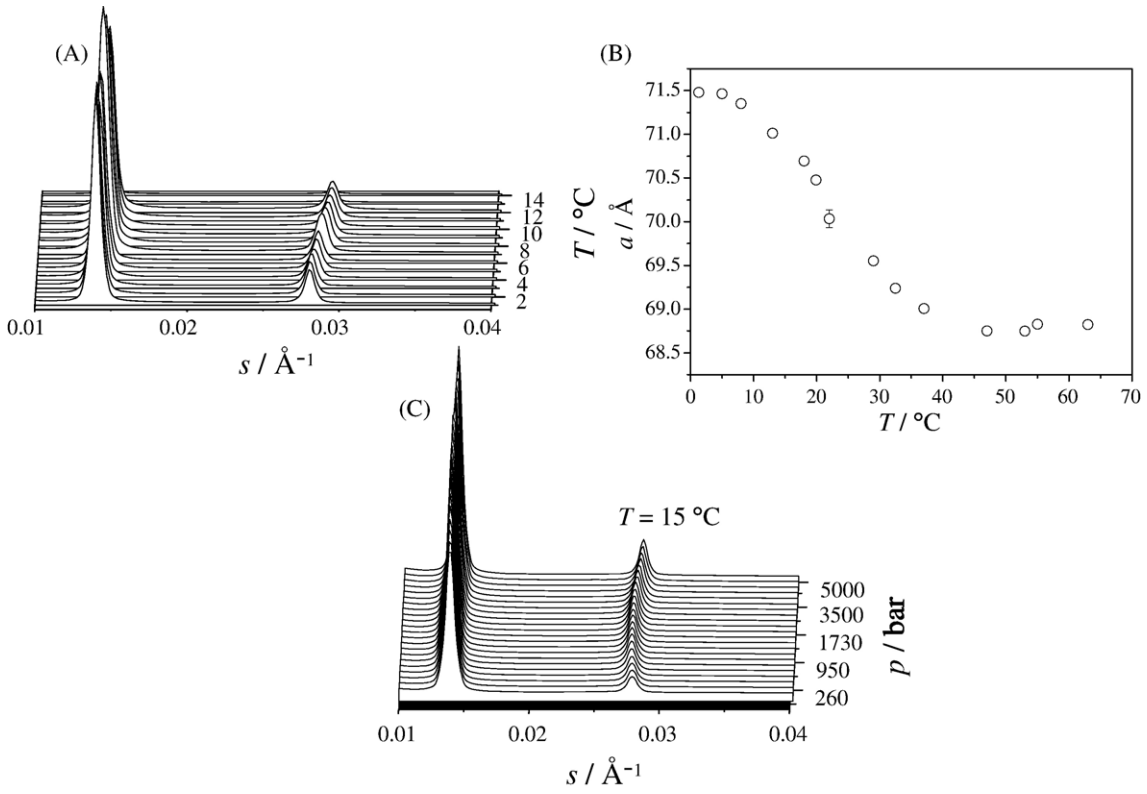

Fig. 3. (A) Small-angle X-ray scattering patterns of POPC/SM/Chol (1:1:1), 20%(w/w), in D_2O during a heating scan from 1.3 to 63 °C. (B) Average lamellar lattice constant *a* of the same lipid mixture as a function of temperature. (C) Small-angle X-ray diffraction patterns of the lipid mixture as a function of pressure measured at 15 °C.

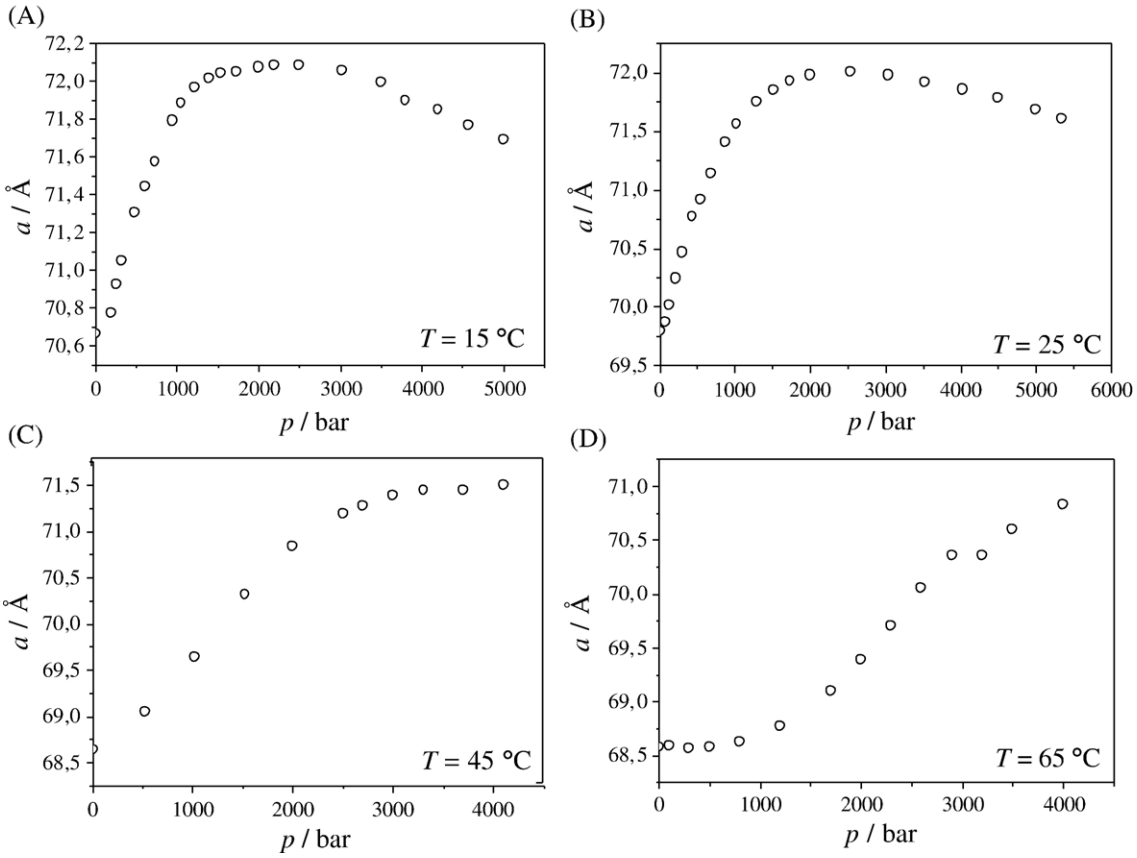

Fig. 4. Average lamellar lattice constant a of POPC/SM/Chol (1:1:1), 20%(w/w), in D_2O during pressure scans from 1 to ~5000 bar at different temperatures (15, 25, 45 and 65 °C).

pressure-induced l_o+l_d to $l_o+l_d+s_o$ transition is detected at 2300±200 bar (Fig. 4C). At 65 °C (Fig. 4D), the l_d to l_d+l_o transition appears at 1200 bar, and the l_o+l_d to $l_o+l_d+s_o$ occurs at 2700 bar as indicated by the change in slope of a (p). In many cases, characteristic changes also appeared in the half widths of the Bragg reflections at the transition pressures, which have therefore also been used in the identification of phase changes (data not shown).

3.3. Differential scanning and pressure perturbation calorimetry (DSC/PPC) data

Additional DSC and PPC studies were carried out from 5 to 95 °C for different sample compositions. Fig. 5A shows PPC and DSC curves of lipid vesicles in buffer solution (150 mM NaCl, 100 mM sodium phosphate in H_2O, pH 7.4) composed of an equimolar ratio of the lipid mixture POPC/SM/Chol. The DSC and PPC data reveal a transition between 5 and 50–65 °C with a broad maximum appearing at ~20 °C. As already discussed by Heerklotz [34], the interpretation of such a broad peak is not straightforward. According to the FT-IR and SAXS data, this broad peak corresponds to the transition from the $l_d+l_o+s_o$ three phase region to the l_o+l_d two-phase coexistence region, reaching an overall l_d state above about 55 °C. Please note that due to the H_2O/D_2O isotope effect, there will be a difference of a few degrees in the phase transition temperatures with respect to the FT-IR and SAXS data, which were obtained for D_2O as solvent. An integration of the DSC and PPC peaks to determine an overall enthalpy change (ΔH) and volume change (ΔV), respectively, for this sample is hampered by the problem of computing a baseline in the low temperature region.

Fig. 5B displays the data for the 2:1:1 POPC/SM/Chol mixture. For this lipid mixture, which contains more fluidizing lipid POPC, the overall fluid phase is reached already at about 40 °C. The DSC and PPC data of the 3:3:1 and 2.5:6.5:1 lipid mixture, having an increasing SM content, which has a strong ordering effect on the acyl chains, are displayed in Fig. 5C and D, respectively. The maxima due to the $l_d+l_o+s_o$ to l_o+l_d transition appear at 25 °C and 32 °C for the 3:3:1 and 2.5:6.5:1 lipid mixtures, respectively. For the latter mixture, a pretransitional peak is visible, which is probably due to the transition from an overall ordered l_o+s_o to $l_d+l_o+s_o$ transition. Notably, for all lipid mixtures, the overall fluid-like, liquid-disordered state is reached at a rather similar temperature region of about 40–55 °C.

Interestingly, the shapes of the DSC and PPC curves, which are overlaid here, indicate that the statistical–mechanical fluctuations probed by these measurements, are strongly related. Enthalpy and volume fluctuations are given by the relevant

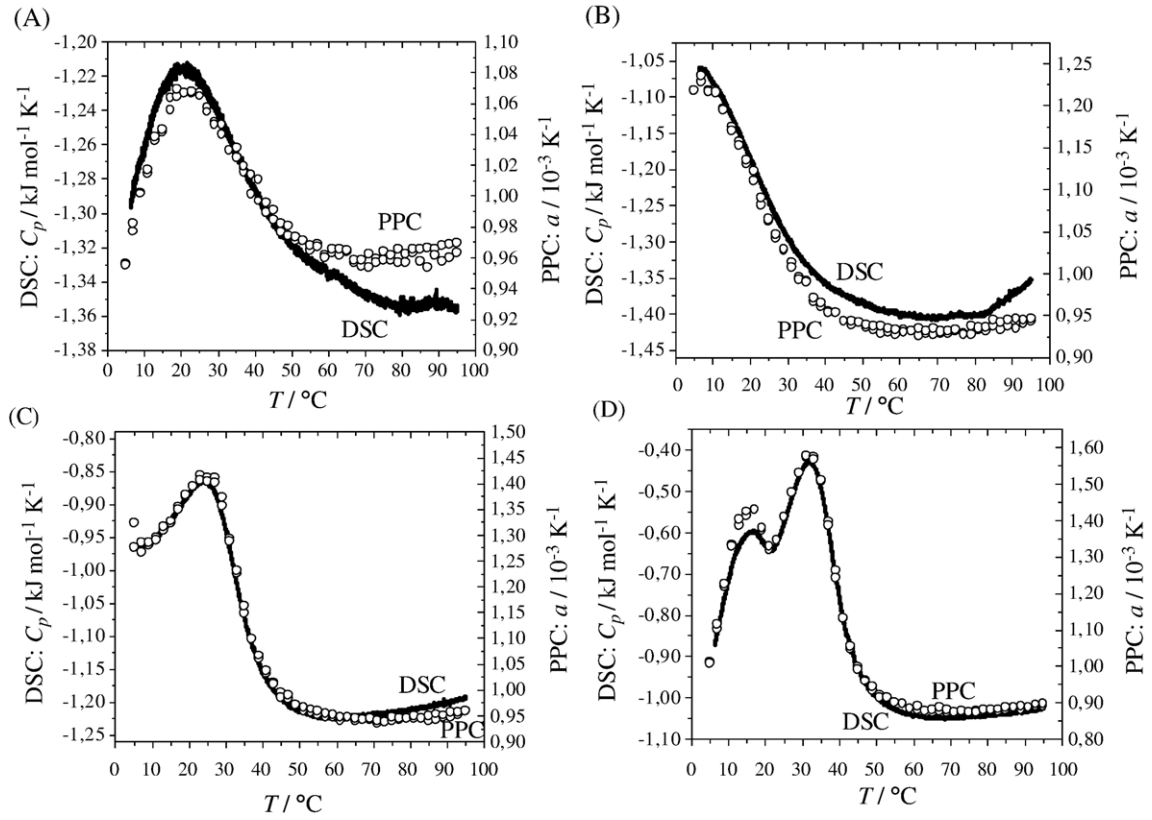

Fig. 5. (A) DSC (left axis, solid line) and PPC (right axis, ○) data of POPC/SM/Chol (1:1:1) in 150 mM NaCl, 100 mM sodium phosphate in H_2O, pH 7.4. (B), (C) and (D) correspond to DSC and PPC curves for the molar ratios 2:1:1, 3:3:1 and 2.5:6.5:1 of POPC/SM/Chol, respectively.

susceptibilities, the heat capacity C_p at constant pressure and the isothermal compressibility β_T as and $\langle(\Delta H)^2\rangle = k_B T^2 m C_p$ and $\langle(\Delta V)^2\rangle = k_B T V \beta_T$, respectively [60,61]. Here, k_B is the Boltzmann constant and V and m are the volume and mass of the lipid, respectively. Combined enthalpy and volume fluctuations are related to the coefficient of thermal expansion, $<(\Delta H)(\Delta V)> = k_B T^2 V \alpha$ [60,61].

Recently, Heimburg et al. found [62–64] that the volume expansion coefficient of single lipid membranes has a very similar temperature dependence as the heat capacity. On the basis of their densimetric experiments, they have argued that this may lead to a simple relation between heat capacity and isothermal volume compressibility. As indicated above, the heat capacity is proportional to enthalpy fluctuations, whereas the compressibility is proportional to volume fluctuations. Thus, if enthalpy and volume are closely related, enthalpy and volume fluctuations supposedly are also related functions of the temperature and are coupled functions. Furthermore, they have suggested that a similar close relationship may exist between lipid area and enthalpy fluctuations. Moreover, it has been concluded that heat capacity and elastic constants are generally closely related. The proportional constant found was the same for all lipids investigated in these studies, including even complex biological mixtures [62–64].

It should be noted that such proportionality relations, like that between enthalpy and volume changes at phase transitions, are probably not universal for order–disorder transitions. The origin of such simple relationships in lipid systems may be due to the fact that the predominant part of the fluctuating properties in lipids are largely due to internal degrees of freedom of the individual lipid molecules, such as trans-gauche isomerizations, and are less influenced by intermolecular contributions.

As revealed by the PPC data, the relative volume changes $\Delta V/V$ at the l_o+s_o to $l_d+l_o+s_o$ and the $l_d+l_o+s_o$ to l_d+l_o transitions are of the order of 0.3% and 0.8%, respectively. The corresponding heat capacity changes for these transitions amount about 15 and 10 kJ/mol, respectively. For comparison, the relative volume and enthalpy changes at the gel to fluid transition of phospholipid bilayers are much larger. For simple, one-component phospholipid membranes undergoing a melting transition, changes in enthalpy by 20–40 kJ/mol and in volume by about 3–4% are observed [1,2,65].

3.4. Temperature and pressure dependent Laurdan fluorescence spectroscopy measurements

We first discuss the temperature dependence of the generalized polarization function, *GP*, of the Laurdan labeled ternary lipid mixture at ambient pressure. Fig. 6A depicts *GP* values of the system POPC/SM/Chol (1:1:1) measured over a temperature range from 3 to 75 °C. As can be clearly seen, the generalized polarization value gradually decreases with increasing temperature, with a sigmoidal kind of shape in the temperature interval between 15 and 65 °C.

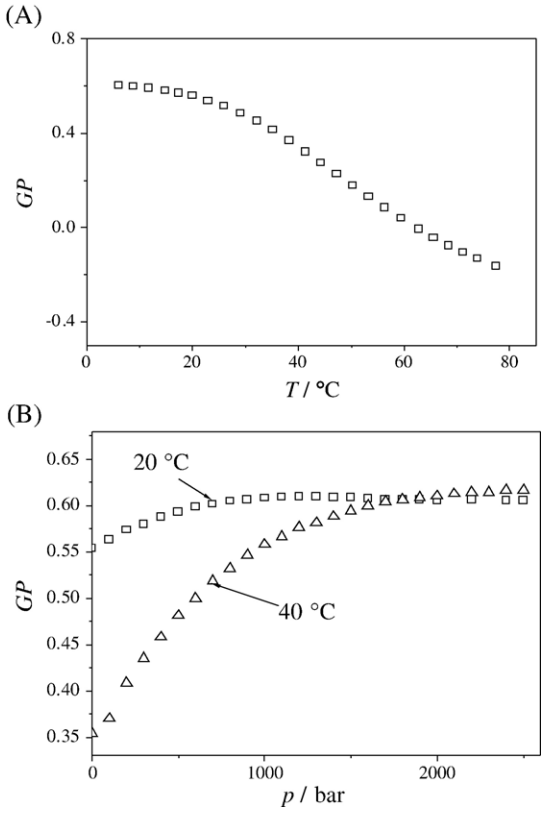

Fig. 6. (A) Temperature and (B) pressure dependence (at 20 and 40 °C) of Laurdan *GP* values of the lipid mixture POPC/SM/Chol (1:1:1).

In fact, a rather smooth and broad transitional behavior is expected from Gibbs' phase rule for such phase transitions of three-component lipid mixtures. This case is very different from the one of one-component lipid bilayer membranes, which generally exhibit rather sharp gel-to-gel and a gel-to-fluid phase transitions [1,2]. By a more or less continuous increase of liquid-disordered domains, the fluidity and conformational disorder of the membrane gradually increases with increasing temperature, and a *GP* value of −0.2 is reached at ∼80 °C. No clear-cut value for the transition temperature to the overall fluid phase can be given, owing to the continuous nature of the *GP* curves, however.

The effect of pressure on the generalized polarization data of the Laurdan labeled POPC/SM/Chol (1:1:1) mixture is shown in Fig. 6B, which exhibits *GP* data measured at two different temperatures (T=20 °C and T=40 °C) as a function of pressure, from 1 up to 2500 bar. At T=20 °C, the *GP* values increase steadily with increasing pressure up to about 1.1 kbar. At the *GP* value of ∼0.60, a plateau is reached, indicating the presence of a rather ordered state, probably a s_o+l_o phase, which is not affected upon application of higher pressures up to the maximum pressure of 2.5 kbar applied here. At much higher pressures, the transition to an all s_o phase could be envisaged. A corresponding *GP* plateau value of ∼0.62 is reached around ∼2.4 kbar at T=40 °C, which suggests the formation of an all-ordered phase at that temperature. Please note that the maximal *GP* values (0.605 at T=20 °C and 0.616 at T=40 °C) reached upon pressurization are only slightly larger than that (0.602) at the lowest temperature (6 °C) of the system at ambient pressure. Hence, a temperature decrease of about 40 °C has a similar effect on membrane ordering and lateral organization as a pressure increase of about 1 kbar at room temperature (T=20 °C) and of ∼2 kbar at 40 °C, respectively (Fig. 7).

4. Conclusions

Fourier-transform infrared spectroscopy in combination with DSC, PPC, fluorescence spectroscopy and synchrotron X-ray scattering has been used to characterize temperature and pressure dependent changes in the conformation, hydration, structure and phase behavior of the canonical lipid raft mixture POPC/SM/Chol (1:1:1), and to establish a *T*, *p*-phase diagram of the system in excess water over an extended temperature and pressure range. A tentative stability phase diagram as obtained from the combined results of all methods applied has been constructed, which is depicted in Fig. 7. The data for the all-fluid to liquid-ordered/liquid-disordered phase transition may be compared with the slope of ∼20 °C/kbar for the pressure-induced fluid to gel phase transition of one-component lipid bilayer systems [39–41].

We realize that the liquid-disordered/liquid-ordered (+solid-ordered) phase coexistence region of the POPC/SM/Chol (1:1:1) model raft mixture extends over a rather wide temperature range of about 40 °C. An overall fluid phase is reached at rather high temperatures (above ∼50 °C), only. Upon pressurization at room temperature (20 °C), an overall (liquid- and solid-) ordered membrane state with high ordering of their acyl chains is reached at pressures of about 1 kbar. A temperature decrease of about 40 °C has a similar effect on membrane ordering and lateral organization as a pressure increase of about 1 kbar at room temperature. At 40 °C, the

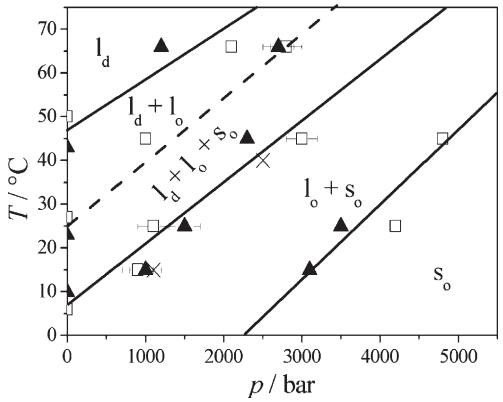

Fig. 7. Tentative *T*, *p*-phase diagram of POPC/SM/Chol (1:1:1) dispersions as obtained from the FT-IR spectroscopy (□) and SAXS (▲) data. In addition, data from fluorescence spectroscopy (X) are included. The l_o+l_d/l_o+l_d+s transition line is difficult to determine precisely and has therefore been plotted as dashed line.

l_o+s_o ordered lipid state of the POPC/SM/Chol (1:1:1) mixture is reached at ~2 kbar. Interestingly, in this pressure range of 2 kbar, ceasing of membrane protein function in natural membrane environments has been observed for a variety of systems (36–38,48,49,52), which might be correlated with the membrane matrix reaching a physiologically unacceptable overall ordered state at these pressures. Moreover, many bacterial organisms have been shown to completely loose activity at these pressures ([36,7–38] and refs. therein).

Acknowledgements

Financial support from the Deutsche Forschungsgemeinschaft and the Fonds der Chemischen Industrie is gratefully acknowledged.

References

[1] G. Cevc (Ed.), Phospholipids Handbook, Marcel Dekker, New York, 1993.
[2] R.M. Epand (Ed.), Lipid polymorphism and membrane properties, Current Topics in Membranes, vol. 44, Academic Press, San Diego, 1997.
[3] R. Lipowski, E. Sackmann (Eds.), Structure and Dynamics of Membranes, vols. 1A, 1B, Elsevier, Amsterdam, 1995.
[4] J.M. Seddon, Structure of the inverted hexagonal (HII) phase, and non-lamellar phase transitions of lipids, Biochim. Biophys. Acta 1031 (1990) 1–69.
[5] J.M. Seddon, R.H. Templer, Cubic phases of self-assembled amphiphilic systems, Philos. Trans. R. Soc. London, Ser. 344 (1993) 377–401.
[6] O.G. Mouritsen, Life as a Matter of Fat. The Emerging Science of Lipidomics, Springer-Verlag, Heidelberg, 2005.
[7] D. Needham, T.J. McIntosh, E. Evans, Thermomechanical and transition properties of dimyristoylphosphatidylcholine/cholesterol bilayers, Biochemistry 27 (1988) 4668–4673.
[8] P.F.F. Almeida, W.L.C. Vaz, T.E. Thompson, Percolation and diffusion in three-component lipid bilayers: effect of cholesterol on an equimolar mixture of two phosphatidylcholines, Biophys. J. 64 (1993) 399–412.
[9] K. Simons, G. van Meer, Lipid sorting in epithelial cells, Biochemistry 27 (1988) 6197–6202.
[10] R. Winter, C. Czeslik, Pressure effects on the structure of lyotropic lipid mesophases and model biomembrane systems, Z. Kristallogr. 215 (2000) 454–474.
[11] J.H. Ipsen, G. Karlström, O.G. Mouritsen, H. Wennerström, M.J. Zuckermann, Phase equilibria in the phosphatidylcholine–cholesterol system, Biochim. Biophys. Acta 905 (1987) 162–172.
[12] J.H. Ipsen, O.G. Mouritsen, M.J. Zuckermann, Theory of thermal anomalies in the specific heat of lipid bilayers containing cholesterol, Biophys. J. 56 (1989) 661–667.
[13] R.F.M. de Almeida, A. Fedorov, M. Prieto, Sphingomyelin/phosphatidylcholine/cholesterol phase diagram: boundaries and composition of lipid rafts, Biophys. J. 85 (2003) 2406–2416.
[14] R.F.M. de Almeida, L.M.S. Loura, A. Fedorov, M. Prieto, Lipid rafts have different sizes depending on membrane composition: a time-resolved fluorescence resonance energy transfer study, J. Mol. Biol. 346 (2005) 1109–1120.
[15] N. Kahya, D. Scherfeld, K. Bacia, B. Poolman, P. Schwille, Probing lipid mobility of raft-exhibiting model membranes by fluorescence correlation spectroscopy, J. Biol. Chem. 278 (2003) 28109–28115.
[16] S.L. Veatch, S.L. Keller, A closer look at the canonical 'raft mixture' in model membrane studies, Biophys. J. 84 (2003) 725–726.
[17] S.L. Veatch, S.L. Keller, Organization in lipid membranes containing cholesterol, Phys. Rev. Lett. 89 (2002) 268101.
[18] K. Simons, W.L.C. Vaz, Model systems, lipid rafts, and cell membranes, Annu. Rev. Biophys. Biomol. Struct. 33 (2004) 269–295.
[19] R.G.W. Anderson, K. Jacobson, A role for lipid shells in targeting proteins to caveolae, rafts, and other lipid domains, Science 296 (2002) 1821–1825.
[20] M. Edidin, The state of lipid rafts: from model membranes to cells, Ann. Rev. Biophys. Biomol. Struct. 32 (2003) 257–283.
[21] S. Munro, Lipid rafts: elusive or illusive? Cell 115 (2003) 377–388.
[22] P.T.T. Wong, D.J. Siminovitch, H.H. Mantsch, Structure and properties of model membranes: new knowledge from high-pressure vibrational spectroscopy, Biochim. Biophys. Acta 947 (1988) 139–171.
[23] M. Auger, H.C. Jarrell, I.C.P. Smith, D.J. Siminovitsch, H.H. Mantsch, P.T.T. Wong, Effects of the local anesthetic tetracaine on the structural and dynamic properties of lipids in model membranes: a high-pressure Fourier transform infrared study, Biochemistry 27 (1988) 6086–6093.
[24] A. Nilsson, A. Holmgren, G. Lindblom, FTIR study of lamellar and reversed micellar phases in the mono-oleoylglycerol/water system, Chem. Phys. Lipids 69 (1994) 219–227.
[25] J. Tuchtenhagen, W. Ziegler, A. Blume, Acyl chain conformational ordering in liquid-crystalline bilayers: comparative FT-IR and 2H-NMR studies of phospholipids differing in headgroup structure and chain length, Eur. Biophys. J. 23 (1994) 323–335.
[26] R. Mendelsohn, M.A. Davies, J.W. Brauner, H.F. Schuster, R.A. Dluhy, Quantitative determination of conformational disorder in the acyl chains of phospholipid bilayers by infrared spectroscopy, Biochemistry 28 (1989) 8934–8939.
[27] M.A. Davies, H.F. Schuster, J.W. Brauner, R. Mendelsohn, Effects of cholesterol on conformational disorder in dipalmitoylphosphatidylcholine bilayers. A quantitative IR study of the depth dependence, Biochemistry 29 (1990) 4368–4373.
[28] H.H. Mantsch, R.N. McElhaney, Phospholipid phase transitions in model and biological membranes as studied by infrared spectroscopy, Chem. Phys. Lipids 57 (1991) 213–226.
[29] H.L. Casal, R.N. McElhaney, Quantitative determination of hydrocarbon chain conformational order in bilayers of saturated phosphatidylcholines of various chain lengths by Fourier transform infrared spectroscopy, Biochemistry 29 (1990) 5423–5427.
[30] A. Blume, W. Hübner, G. Messner, Fourier transform infrared spectroscopy of $^{13}C{=}O$-labeled phospholipids hydrogen bonding to carbonyl groups, Biochemistry 27 (1988) 8239–8249.
[31] R.N. Lewis, R.N. McElhaney, W. Pohle, H.H. Mantsch, Components of the carbonyl stretching band in the infrared spectra of hydrated 1,2-diacylglycerolipid bilayers: a reevaluation, Biophys. J. 67 (1994) 2367–2375.
[32] O. Reis, R. Winter, T.W. Zerda, The effect of high external pressure on DPPC-cholesterol multilamellar vesicles—A pressure-tuning Fourier-transform infrared spectroscopy study, Biochim. Biophys. Acta 1279 (1996) 5–16.
[33] R. Winter, R. Köhling, Static and time-resolved synchrotron small-angle X-ray scattering studies of lyotropic lipid mesophases, model biomembranes and proteins in solution, J. Phys.: Condens. Matter 16 (2004) S327–S352.
[34] H. Heerklotz, J. Seelig, Application of pressure perturbation calorimetry to lipid bilayers, Biophys. J. 82 (2002) 1445–1452;
H. Heerklotz, Triton promotes domain formation in lipid raft mixtures, Biophys J. 83 (2002) 2693–2701.
[35] R. Ravindra, R. Winter, Pressure perturbation calorimetric studies of the solvation properties and the thermal unfolding of proteins in solution, Z. Phys. Chem. 217 (2003) 1221–1243.
[36] C. Balny, P. Masson, K. Heremans, High pressure effects on biological macromolecules: from structural changes to alteration of cellular processes, Biochim. Biophys. Acta 1595 (2002) 3–10.
[37] H. Ludwig, Advances in High Pressure Bioscience and Biotechnology, Springer-Verlag, Heidelberg, 1999.
[38] R. Winter (Ed.), Advances in High Pressure Bioscience and Biotechnology II, Springer-Verlag, Heidelberg, 2003.
[39] R. Winter, W. Dzwolak, Temperature–pressure configurational landscape of lipid bilayers and proteins, Cell. Mol. Biol. 50 (2004) 397–417.
[40] R. Winter, W.C. Pilgrim, A SANS study of high pressure phase transitions in model biomembranes, Ber. Bunsenges. Phys. Chem. 93 (1989) 708–717.
[41] C. Czeslik, O. Reis, R. Winter, G. Rapp, Effect of high pressure on the

structure of dipalmitoylphosphatidylcholine bilayer membranes: a synchrotron-X-ray diffraction and FT-IR spectroscopy study using the diamond anvil technique, Chem. Phys. Lipids 91 (1998) 135–144.
[42] J. Jonas (Ed.), High Pressure NMR, Springer-Verlag, Berlin, 1991.
[43] X. Peng, A. Jonas, J. Jonas, One and two dimensional ^{1}H-NMR studies of pressure and tetracaine effects on sonicated phospholipid vesicles, Chem. Phys. Lipids 75 (1995) 59–69.
[44] L.F. Braganza, D.L. Worcester, Hydrostatic pressure induces hydrocarbon chain interdigitation in single-component phospholipid bilayers, Biochemistry 25 (1986) 2591–2596.
[45] D.C. Fiech, B.B. Bonev, M.R. Morrow, Effect of pressure on dimyristoylphosphatidylcholine headgroup dynamics, Phys. Rev., E 57 (1998) 3334–3343.
[46] B.B. Bonev, M.R. Morrow, ^{2}H NMR studies of dipalmitoylphosphatidylcholine and dipalmitoylphosphatidylcholine–cholesterol bilayers at high pressure, Can. J. Chem. 76 (1998) 1512–1519.
[47] M. Zein, R. Winter, Effect of temperature, pressure and lipid acyl-chain length on the structure and phase behaviour of phospholipid–gramicidin bilayers, Phys. Chem. Chem. Phys. 2 (2000) 4545–4551.
[48] P.L. Chong, P.A. Fortes, D.M. Jameson, Mechanisms of inhibition of (Na,K)-ATPase by hydrostatic pressure studied with fluorescent probes, J. Biol. Chem. 260 (1985) 14484–14490.
[49] S. Janosch, E. Kinne-Saffran, R.K.H. Kinne, R. Winter, Inhibition of Na^{+}, K^{+}-ATPase by hydrostatic pressure, in: R. Winter (Ed.), Advances in High Pressure Bioscience and Biotechnology II, Springer-Verlag, Heidelberg, 2003, pp. 215–219.
[50] S. Scarlata, Determination of the activation volume of PLCβ by Gβγ-subunits through the use of high hydrostatic pressure, Biophys. J. 88 (2005) 2867–2874.
[51] S. Scarlata, The effect of hydrostatic pressure on membrane-bound proteins, Braz. J. Med. Biol. Res. 38 (2005) 1203–1208.
[52] H.M. Ulmer, H. Herberhold, S. Fahsel, M.G. Gänzle, R. Winter, R.F. Vogel, Effects of pressure-induced membrane phase transitions on inactivation of HorA, an ATP-dependent multidrug resistance transporter, in *Lactobacillus plantarum*, Appl. Environ. Microbiol. 68 (2002) 1088–1095.
[53] G. Panick, R. Malessa, R. Winter, G. Rapp, K.J. Frye, C. Royer, Structural characterization of the pressure-denatured state and unfolding/refolding kinetics of staphylococcal nuclease by synchrotron small-angle X-ray scattering and Fourier-transform infrared spectroscopy, J. Mol. Biol. 275 (1998) 389–402.
[54] D.J. Siminovitch, P.T.T. Wong, H.H. Mantsch, Effects of cis and trans unsaturation on the structure of phospholipid bilayers: a high-pressure infrared spectroscopic study, Biochemistry 26 (1987) 3277–3287.
[55] J. Kraineva, R.A. Narayanan, E. Kondrashkina, P. Thiyagarajan, R. Winter, Kinetics of lamellar-to-cubic and intercubic phase transitions of pure and cytochrome *c* containing monoolein dispersions monitored by time-resolved small-angle X-ray diffraction, Langmuir 21 (2005) 3559–3571.
[56] R. Ravindra, R. Winter, Pressure perturbation calorimetry: a new technique provides surprising results on the effects of co-solvents on protein solvation and unfolding behavior, ChemPhysChem 5 (2004) 566–571.
[57] T. Parasassi, G. de Stasio, A. d'Ubaldo, E. Gratton, Phase fluctuation in phospholipid membranes revealed by Laurdan fluorescence, Biophys. J. 57 (1990) 1179–1186.
[58] O. Reis, R. Winter, Pressure and temperature effects on conformational and hydrational properties of lamellar and bicontinuous cubic phases of the fully hydrated monoacylglyceride monoelaidin—A Fourier transform-infrared spectroscopy study using the diamond anvil technique, Langmuir 14 (1998) 2903–2909.
[59] M.C.R. Symons, G. Eaton, Solvation of acetone in protic and aprotic solvents and binary solvent mixtures, J. Chem. Soc., Faraday Trans. 1 81 (1985) 1963–1977.
[60] T.L. Hill, An Introduction to Statistical Thermodynamics, Addison-Wesley, 1960.
[61] A. Cooper, Protein fluctuations and the thermodynamic uncertainty principle, Prog. Biophys. Mol. Biol. 44 (1984) 181–214.
[62] H. Ebel, P. Grabitz, T. Heimburg, Enthalpy and volume changes in lipid membranes I. The proportionality of heat and volume changes in the lipid melting transition and its implication for the elastic constants, J. Phys. Chem., B 105 (2001) 7353–7360.
[63] W. Schrader, H. Ebel, P. Grabitz, E. Hanke, T. Heimburg, M. Hoeckel, M. Kahle, F. Wente, U. Kaatze, Compressibility of lipid mixtures studied by calorimetry and ultrasonic velocity measurements, J. Phys. Chem., B 106 (2002) 6581–6586.
[64] H.M. Seeger, M. Fidorra, T. Heimburg, Domain size and fluctuations at domain interfaces in lipid mixtures, Macromol. Symp. 219 (2005) 85–96.
[65] M. Böttner, D. Ceh, U. Jakobs, R. Winter, High pressure volumetric measurements on phospholipid bilayers, Z. Phys. Chem. 184 (1994) 205–218.